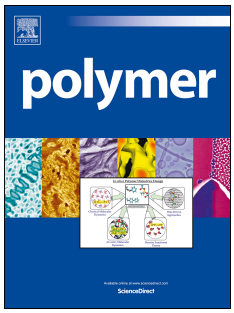

Electrospun Thermoplastic Polyurethane Membrane Decorated with Carbon Nanotubes: A Platform of Flexible Strain Sensors for Human Motion Monitoring

Zijian Wu, Xuesong Deng, Xin Yu, Junwei Gu, Zeinhom M. El-Bahy, Gaber A.M. Mersal, Jing Zhang, A. Alhadhrami, Hongyu Xu, Ning Guo, Junguo Gao, Ling Weng, Zhanhu Guo

PII: S0032-3861(24)00456-7

DOI: https://doi.org/10.1016/j.polymer.2024.127120

Reference: JPOL 127120

To appear in: *Polymer*

Received Date: 18 March 2024

Revised Date: 28 April 2024

Accepted Date: 1 May 2024

Please cite this article as: Wu Z, Deng X, Yu X, Gu J, El-Bahy ZM, Mersal GAM, Zhang J, Alhadhrami A, Xu H, Guo N, Gao J, Weng L, Guo Z, Electrospun Thermoplastic Polyurethane Membrane Decorated with Carbon Nanotubes: A Platform of Flexible Strain Sensors for Human Motion Monitoring, *Polymer*, https://doi.org/10.1016/j.polymer.2024.127120.

Graphical Abstract

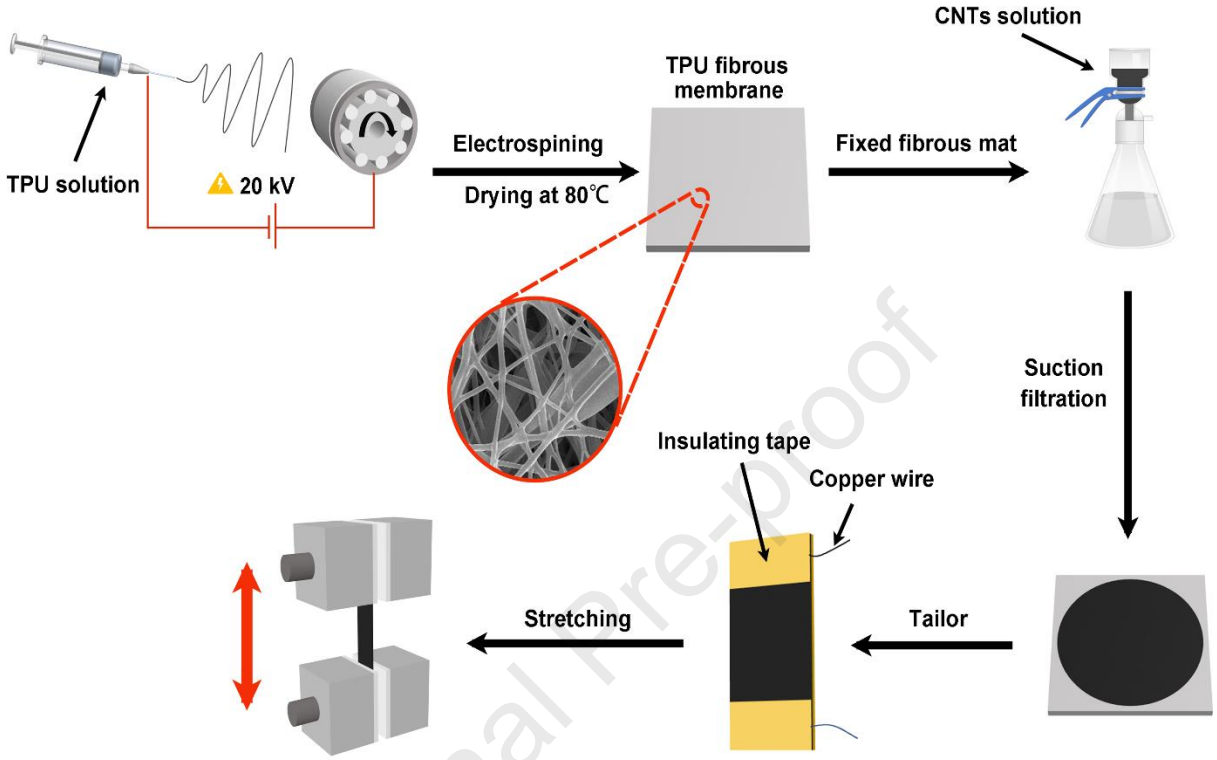

Electrospun Thermoplastic Polyurethane Membrane Decorated with Carbon Nanotubes: A Platform of Flexible Strain Sensors for Human Motion Monitoring

Zijian Wu,[a,b,c] Xuesong Deng,[a] Xin Yu,[d] Junwei Gu,[e] Zeinhom M. El-Bahy,[g] Gaber A. M. Mersal,[h] Jing Zhang,[c,f] A. Alhadhrami[h], Hongyu Xu, [a] Ning Guo,[a,b,*] Junguo Gao,[a,b,*] Ling Weng,[a,b,*] and Zhanhu Guo[*c]

[a] School of Materials Science and Chemical Engineering, Harbin University of Science and Technology, Harbin 150040, China

[b] Key Laboratory of Engineering Dielectric and Its Application Technology of Ministry of Education, Harbin University of Science and Technology, Harbin 150040, China

[c] Mechanical and Construction Engineering, Faculty of Engineering and Environment, Northumbria University, Newcastle Upon Tyne, NE1 8ST UK

[d] Harbin Fiberglass Research Institute Co., Ltd, Harbin 150028, China

[e] Shaanxi Key Laboratory of Macromolecular Science and Technology, School of Chemistry and Chemical Engineering, Northwestern Polytechnical University, Xi'an, Shaanxi, 710072, China

[f] College of Chemical Engineering and Technology, Taiyuan University of Science and Technology, Taiyuan, Shanxi 030024, China

[g] Department of Chemistry, Faculty of Science, Al-Azhar University, Nasr City 11884, Cairo, Egypt

[h] Department of Chemistry, College of Science, Taif University, P.O. Box 11099, Taif 21944, Saudi Arabia

*Corresponding author.

Email: tad@hrbust.edu.cn (N. Guo); gaojunguo@hrbust.edu.cn (J. Gao)

l.weng@hrbust.edu.cn (L. Weng); zhanhu.guo@northumbria.ac.uk (Z.Guo)

Abstract

A piezoresistive flexible strain sensor was developed using thermoplastic polyurethane elastomers (TPU) as the matrix and carbon nanotubes (CNTs) as conductive fillers. Sensitivity, strain range, and tensile cycling stability were concurrently considered during its design. Electrospun TPU fiber membranes were prepared via electrospinning in this experiment, with controllable fiber diameter achieved by adjusting the rotational speed of the electrospinning receiving drum. CNTs were incorporated into a flexible polymer substrate through suction filtration to create the strain sensor. The support structure of the electrospun film served as a carrier for uniformly adhering conductive particles. Well-dispersed conductive CNTs could more easily achieve uniform loading through the pore size of the electrospun fiber film, thereby forming a conductive layer. This study initially determined the influence of TPU content in the spinning solution on the morphology of the electrospun membrane. Subsequently, the effects of CNT content and electrospinning receiving drum rotational speed on the microstructure of TPU electrospun membranes were investigated, along with their impact on the microstructure, mechanical properties, and sensing performance of CNTs/TPU (CT) flexible strain sensors. The results indicate that the electrospun fiber membrane prepared under the conditions of TPU mass fraction of 20 wt% and rotational speed of 100 r/min has a larger average fiber diameter and a more stable scaffold structure. The CNTs/TPU (CT) sensor, prepared by filtering 10 mL of CNTs with a concentration of 2 mg/mL, exhibited the best mechanical properties, with a tensile strength and elongation at break of 6.22 MPa and 575%, respectively. Additionally, it demonstrated high sensitivity (GF=420.17 at 200% strain) and excellent durability stability (300 cycle tests), enabling quick and accurate responses to movements of various parts of the human body, thereby meeting the basic usage requirements of flexible strain sensors.

KEYWORDS: Electrospinning; Flexible strain sensor; sensitivity.

1. Introduction

With the rapid development of intelligent wearable device industry [1-7], sensors have received widespread attention from scholars and experts in academia and industry [8-12]. The device that converts external signal stimuli (such as temperature [13, 14], electrochemical biosensing [15], light, humidity [16-18], strain [19], pressure [20, 21], mechanical deformation [22, 23], gas [24-28], biomolecules [29, 30], chemical [31-33], etc.) into detectable electrical signals is called a sensor [34, 35]. Traditional sensors are made of rigid materials [36], which are hard and brittle, difficult to curl, and difficult to fit well with human skin, making them unsuitable for certain specific applications. There is an urgent need to develop stretchable conductors that can maintain stable conductivity even after undergoing large deformations [37]. The flexible strain sensor based on conductive polymer composite (CPC) materials has bending flexibility and good stretching ability, meeting the usage environment of the sensor under bending, folding, and large stretching (strain ≥ 50%) conditions. The flexible strain sensor has broad application prospects in fields such as human motion monitoring [38-40], flexible electronic skin [41-43], biomedicine [44-46], and human-machine interaction [47].

Common flexible strain sensors use flexible polymer materials with excellent tensile properties as substrates, such as polyvinylidene fluoride (PVDF) [48, 49], cellulose [50], polydimethylsiloxane (PDMS) [51-56], thermoplastic polyurethane elastomer (TPU) [57-62], Ecoflex [63], hydrogel [64-68], etc. Common flexible strain sensors typically combine nanometals (such as gold nanoparticles [69], silver nanowires (AgNWs) [70, 71]), carbon nanomaterials (such as carbon black, carbon nanotubes, graphene) [72, 73], MXene [74] etc.) [75-77], conductive polymers (such as PEDOT: PSS, polypyrrole (PPy) [78-80], and polyaniline (PANI) [81]), and other conductive materials with polymer to give composite materials excellent conductivity.

Lower monitoring limits, wide sensing range, and high sensitivity are key performance requirements for

practical usages of the stretchable flexible strain sensors. Lower monitoring limits can meet the sensor's rapid and accurate response when subjected to small strain stimuli, which is of great significance for disease diagnosis and real-time health monitoring, A wider detection range can meet the use of sensors under large strains, while sensitivity can reflect the sensor's response ability to corresponding strains. However, from the current research status, traditional polymer-based piezoresistive flexible strain sensor has problems such as poor cycle stability and insufficient tensile range when the load is repeatedly loaded, because conductive particles cannot be well combined with the flexible polymer substrate.

In addition, it is difficult to prepare flexible strain sensors with both high tensile capacity and high sensitivity, so the practical application range of flexible strain sensors is also limited [82]. Due to the fact that the piezoresistive flexible strain sensor consists of a sensing material and a flexible substrate, the sensing material determines the response reliability, sensitivity, and threshold sensing level of the strain sensor, while the flexible polymer substrate determines the stretchability and detection range of the sensor. Therefore, it is reasonable to choose materials and adjust preparation methods to solve the bonding problem between conductive particles and flexible polymer substrates. The coordinated solution of the mutual matching between sensing performance and tensile performance has become a top priority in research to prepare a piezoresistive flexible strain sensor that takes into account of both high sensitivity and high tensile capacity.

In this study, a flexible TPU substrate was prepared through electrospinning technology [83], and combined conductive particles with the flexible TPU substrate through suction filtration to prepare a flexible strain sensor. Silicone rubber and TPU are the two most common types of polymer matrix materials for flexible strain sensors. Among them, silicone rubber, such as PDMS and Ecoflex, exhibits excellent elasticity, stretchability, and biocompatibility. However, silicone rubber is difficult to prepare via electrospinning process. Therefore, TPU

was chosen as the polymer matrix in this study. The support structure of the electrospun membrane can be used as a carrier for the uniform attachment of conductive particles, and the well dispersed nanotubes can more easily achieve uniform loading by means of suction filtration with the help of the pore size of the electrospun membrane to build a conductive layer. Compared to methods such as chemical grafting, electrostatic adsorption, and polymer solution coating, the vacuum filtration method is more convenient and efficient for introducing CNTs onto the surface of TPU fiber membranes. The prepared flexible polymer substrate demonstrated good mechanical properties by controlling the fiber diameter of the electrospun membrane to meet the basic use needs of the flexible strain sensor. The optimal content of TPU in the spinning solution was first determined, followed by an investigation into the effects of CNTs content and electrospinning receiving drum rotational speed on the microstructure of TPU electrospun membranes, as well as their impact on the microstructure, mechanical properties, and sensing performance of flexible strain sensors.

2. Experimental

2.1 Materials

Thermoplastic polyurethane (TPU Elastollan 1185A, density 1.05 g/cm^3) was provided by BASF Co., Ltd. N, N-dimethylformamide (DMF) and tetrahydrofuran (THF) were purchased from Tianjin Fuyu Fine Chemical Co., Ltd. Carboxylated carbon nanotubes (MWCNTs, diameter from 20 to 40 nm, length less than 5 microns) were purchased from Shenzhen Nanotech Port Co., Ltd.

2.2 Preparation of TPU electrospun membrane

TPU electrospun fiber membrane was prepared using electrospinning technology. Firstly, TPU particles were dissolved with a solute mass fraction of 14wt%, 17wt%, 20wt% and 23wt% in a mixed solution of DMF/THF with a mass ratio of 1:1. After mechanical stirring of the mixture at room temperature for 5 hours, a

uniform spinning solution was obtained. Then, the spinning solution was injected into a 15 mL syringe and used for electrospinning. Aluminum foil was selected as the receiving device for TPU fibers on a roller, with a distance of 20 cm between the needle and the receiving device. Electrospinning was carried out at 20 kV, with a propulsion speed of 1 mL/h, and speeds of 100 r/min, 300 r/min, and 500 r/min, respectively. Finally, the prepared TPU fiber membrane was dried at 80℃ for 5 hours to remove residual organic solvents.

2.3 Preparation of flexible strain sensors based on CNTs/TPU

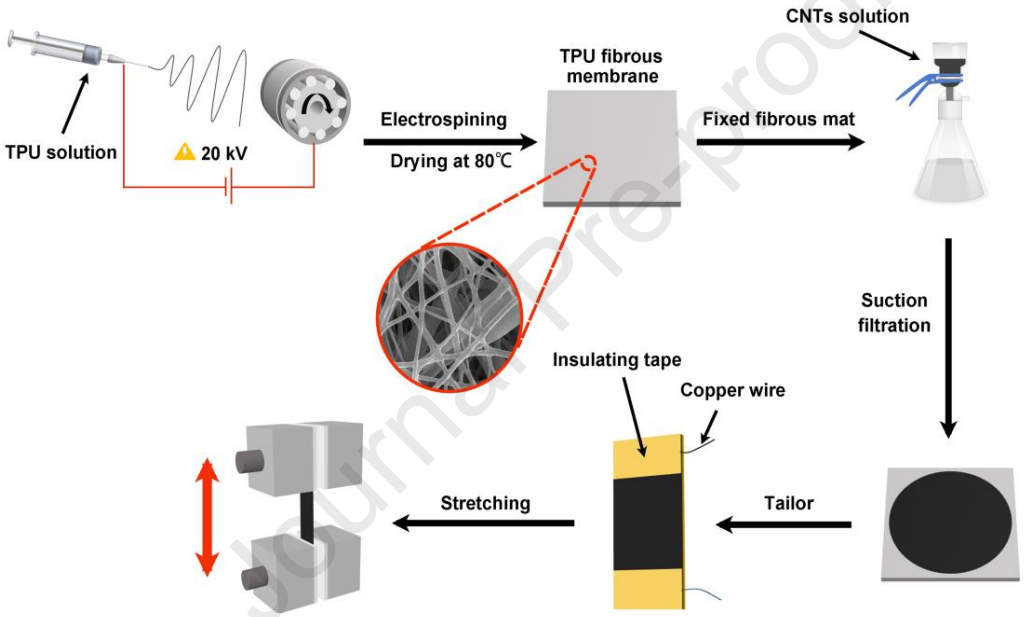

Fig. 1. Preparation process diagram of flexible strain sensors based on CNTs/TPU.

First of all, the TPU fiber film was cut into a size of 50 mm × 50 mm, and the CNTs suspension with a concentration of 2.0 g/L was pumped and filtered on the TPU electrospinning fiber film in the form of 2.5, 5, 7.5, 10 and 15 mL, and rinsed repeatedly with deionized water 3 After that, it was dried in an oven at 80°C. Finally, CNTs/TPU flexible strain sensors were prepared by cutting the TPU fiber film filtered with CNTs into segments of 10 mm × 40 mm and connecting with external wires. For convenience of testing and analysis, the sensors were named as CT series sensors. The preparation process of CNTs/TPU flexible strain sensors is

schematically shown in Fig. 1.

2.4 Fabrication and characterization

Scanning electron microscopy (SEM, Volumescope2, Thermo Scientific, America) was used to observe the morphology of the samples at an accelerating voltage of 5 kV. The tensile tests were performed at room temperature with an electronic universal testing machine (UTM2203, sun, China) equipped with a 2 kN transducer at a rate of 50 mm/min. All samples were rectangular specimens of 40 mm × 10 mm with an applied length of 20 mm. 5 good tests were performed on all specimens and the average value was taken.

The sensing performance of the sensor was characterized using a digital source meter (Keithley 2400) in conjunction with a UTM2203 electronic universal testing machine. A sensor sample of size 40 mm × 10 mm was first fixed on the electronic universal testing machine at a distance of 20 mm from both ends of the fixture, after which the digital source meter was connected to both ends of the sensor and used to test the resistance versus strain of the CT sensors at a constant tensile rate of 10 mm/min. The relative resistance change can be calculated by Equation 1:

$$\Delta R/R_0 = (R - R_0) / R_0 \quad (1)$$

where R_0 is the initial resistance at strain ε=0% and R is the real time resistance when strain is applied.

3. Result and discussion

3.1 The effect of TPU content in spinning solution on the morphology of electrospun membranes

To determine the optimal TPU content in the spinning solution, the TPU electrospun membranes were prepared with TPU mass fractions of 14wt%, 17wt%, 20wt%, and 23wt%, respectively. The morphology of the prepared TPU electrospun membranes was observed via SEM to determine the optimal solute mass fraction for

TPU electrospun membrane fabrication. The SEM images of TPU electrospun membranes with different solute mass fractions magnified by 10,000 times are shown in Fig. 2.

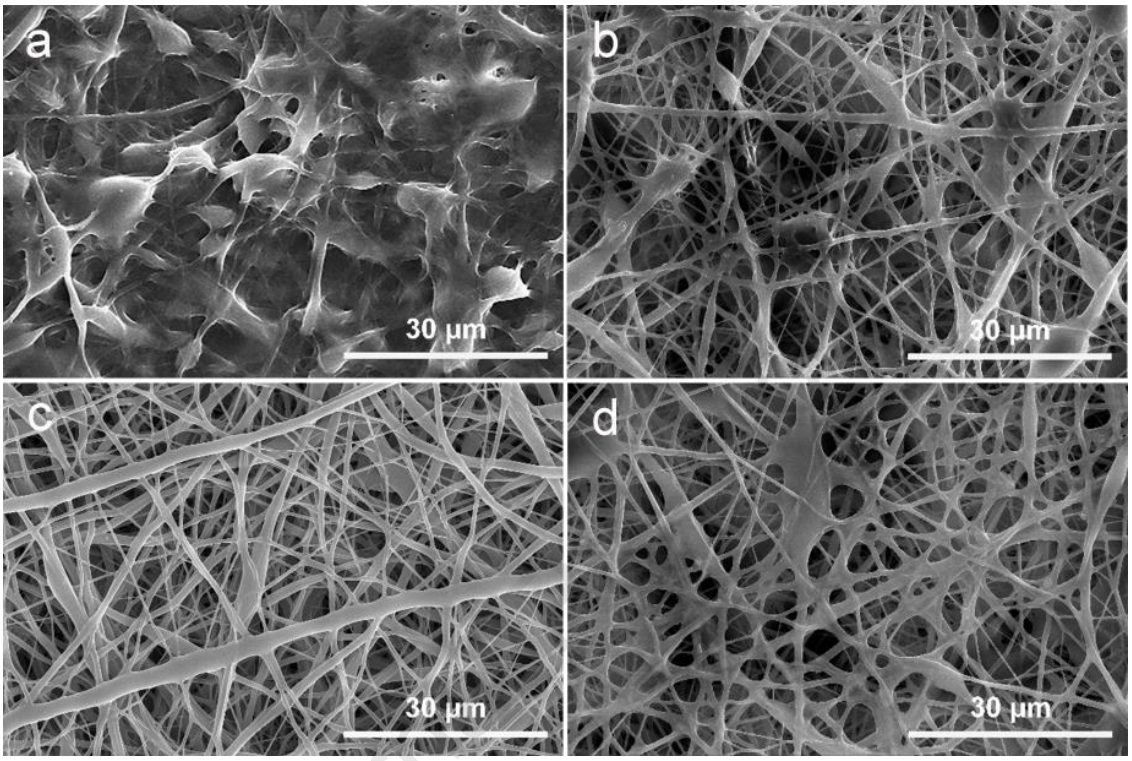

Fig. 2. SEM images of TPU electrospinning film with a solute mass fraction of: **a.**14wt%, **b**. 17wt%, **c**. 20wt%, and **d.** 23wt%

When the TPU mass fraction is 14wt%, no fiber formation occurs on the membrane surface. This is due to the excessively low viscosity arising from the low TPU content in the spinning solution, which prevents the proper jetting. Instead, the spinning solution is ejected in droplet form and lands on the collector. When the TPU mass fraction is increased to 17wt%, fiber structures can be formed on the membrane surface, but there are numerous beading and adhesion between fibers. At this TPU mass fraction, the spinning solution still contains insufficient TPU content, and some droplets fail to jet properly, resulting in beading and adhesion. With a TPU mass fraction of 20wt%, uniform diameter TPU electrospun fiber membranes are successfully produced without

beading or adhesion issues, exhibiting excellent morphology. However, when the TPU mass fraction reaches 23wt%, a small amount of adhesion occurs between the fiber membranes. At this point, the TPU content is too high, resulting in slightly increased viscosity of the spinning solution. This makes it difficult for the solution at the needle tip to overcome surface tension, causing it to directly detach from the needle tip without being stretched by the electric field and drop onto the collection device.

3.2 Performance characterization of CT sensors

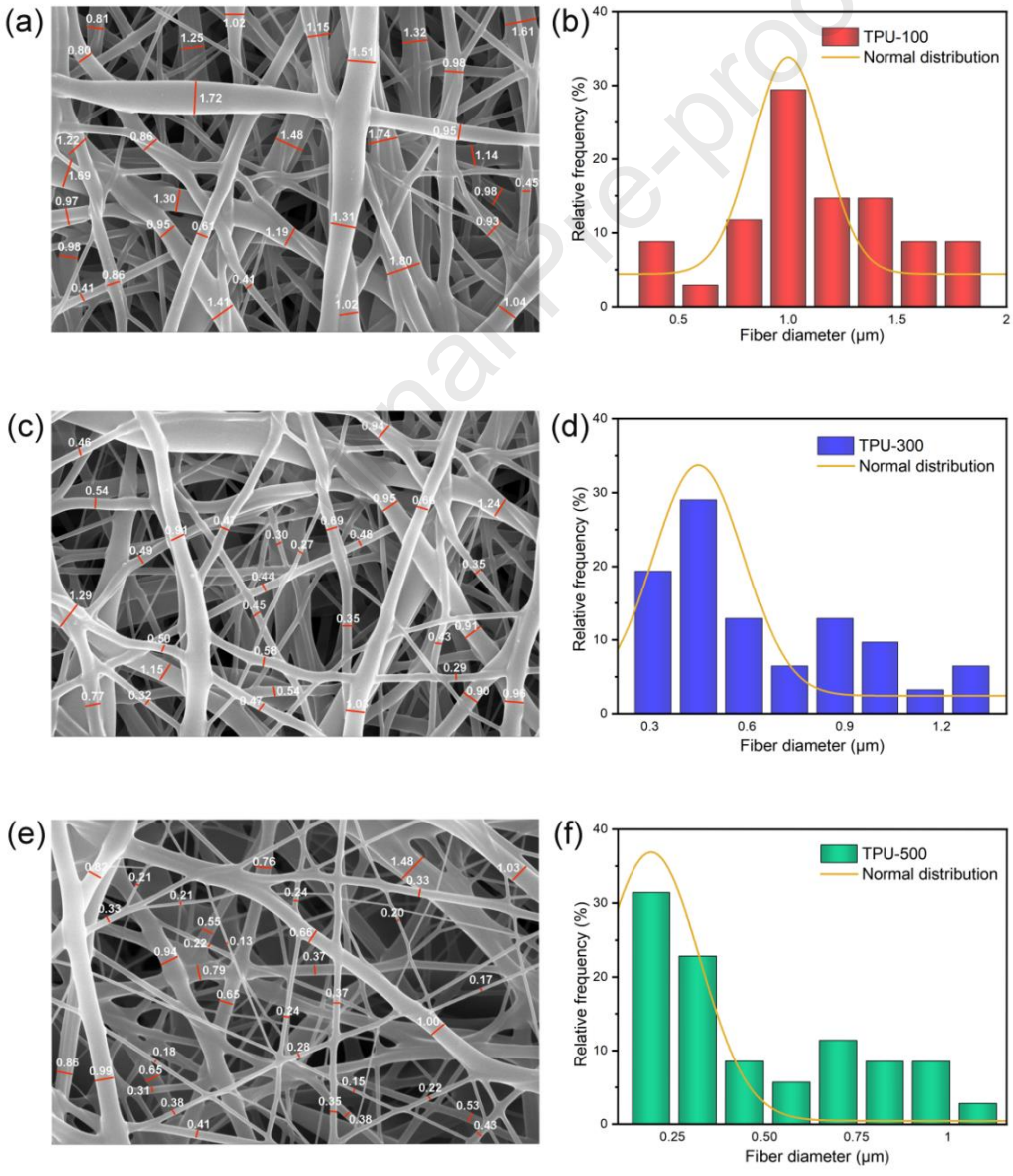

Fig. 3. (a) SEM image of TPU-100. (b) TPU-100 fiber diameter distribution histogram. (c) SEM image of TPU-300. (d) TPU-300 fiber diameter distribution histogram. (e) SEM image of TPU-500. (f) TPU-500 fiber diameter distribution histogram.

The purpose of this experiment is to prepare the optimal TPU electrospun fiber membrane as a flexible polymer substrate. By changing the rotational speed during the electrospinning process, the fiber diameter of the prepared TPU electrospun fiber membrane can be controlled and adjusted [84]. The fiber diameter distribution of the TPU electrospun fiber membrane at different rotational speeds was investigated. The TPU fiber membranes with a mass fraction of 20wt% prepared at 100 r/min, 300 r/min, and 500 r/min were named as TPU-100, TPU-300, and TPU-500, respectively. The fiber diameter distribution of TPU electrospun fiber membranes prepared at various speeds is shown in Fig. 3.

As can be seen from Fig. 3, with the increase of rotational speed in the electrospinning process, the diameters of TPU electrospinning fiber films prepared at three rotational speeds are mainly distributed as 1.10± 0.04 μm, 0.45± 0.03 μm and 0.19± 0.05 μm, respectively, and the relative frequencies gradually decrease. It can be seen that the fine fibers of the prepared TPU electrospun fiber film gradually increase, and the overall fiber diameter distribution tends to decrease, which may be because the collecting device will have stress stretching effect on the fibers during the process of collecting fibers. The higher the rotational speed, the stronger the stress effect, the smaller the fiber diameter. In conclusion, the TPU electrospun fiber film with mass fraction of 20wt% prepared at the rotating speed of 100 r/min has a better surface morphology and a larger fiber diameter.

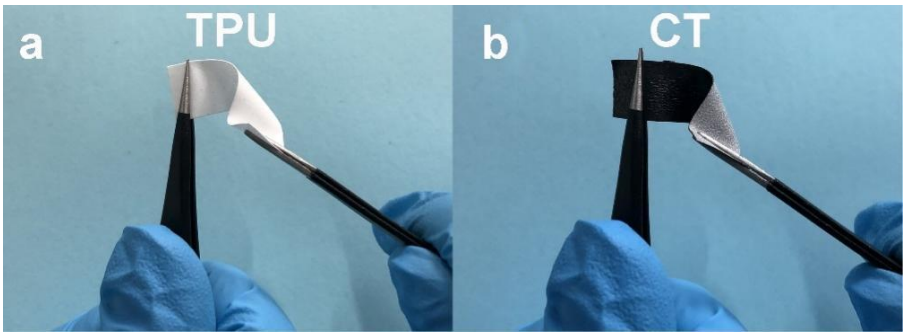

Fig. 4 The optical photographs of TPU nanofiber membranes (a) before and (b) after the filtration of CNTs.

The optical photographs of TPU nanofiber membranes before and after the filtration of CNTs are shown in Fig 4. The SEM images of the CT sensor before and after stretching are shown in Fig 5. The SEM images in Fig 5a and 5b depict the CT sensor before and after stretching and recovery, respectively, magnified by 2000 times.

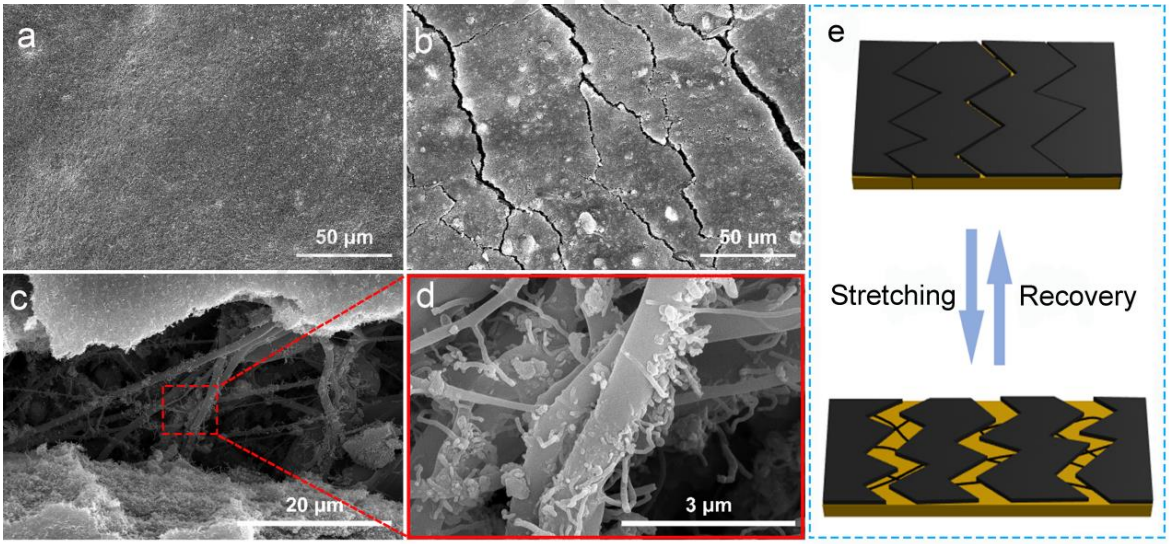

Fig. 5 SEM image of CT sensors. a. without stretching, b. after stretching and recovery, c&d. SEM images of the crack location, e. Schematic diagram of the crack formation process.

From the SEM images, it can be observed that a uniform and dense layer of CNTs conductive layer has been formed on the surface of the TPU fiber membrane. Furthermore, even after stretching and recovery, the

conductive layer composed of CNTs remains tightly interlocked [85]. This ensures the subsequent sensing tests of the CT sensor exhibit a linear change in the relative resistance with the application of strain, providing stability and reliability. Fig 5c and 5d depicts the morphology of the crack locations on the CT sensor magnified by 8000 times and 60000 times, respectively, after stretching. From the images, it can be observed that the TPU fibers at the crack locations are loaded with a certain amount of CNTs. This ensures that even when strain is applied to the CT sensor, the conductive particles can still interconnect, forming a conductive network. This guarantees a wide operating range for the CT sensor.

In this work, the loading capacity of carbon nanotubes determines the conductivity of conductive fiber membranes [86, 87]. The loading amount of CNTs was controlled by filtering 2.5 mL, 5 mL, 7.5 mL, 10 mL, and 15 mL CNTs suspensions with a concentration of 2 g/L onto TPU fiber membranes. The electrical signal responses of CT sensors with different CNTs filtration contents under 10%, 30%, and 50% strain cycles are shown in Fig 6.

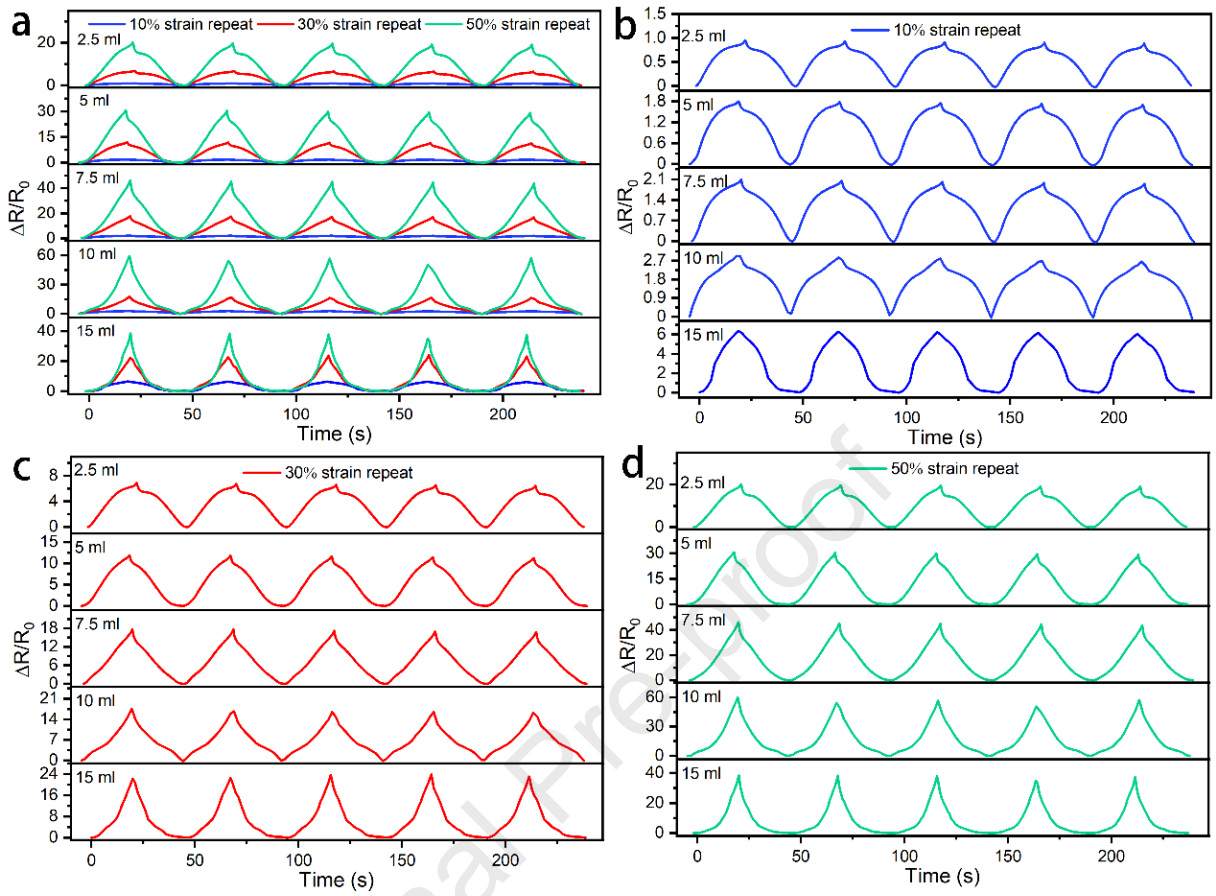

Fig. 6. Cyclic electrical signal response of CT sensors. a. Overall electrical signal response, b. 10% strain cyclic electrical signal response, c. 30% strain cyclic electrical signal response, and d. 50% strain cyclic electrical signal response

Fig. 6a shows the overall electrical signal response of the CT sensors, and the electrical signals of the CT sensor show regular periodic changes under various CNTs loads. As shown in Fig. 6b and 6c, the relative resistance of the CT sensor increases with the increase of CNTs load at 10% and 30% strain. As shown in Fig. 6d, the maximum relative resistance of the CT sensor with 15 mL of CNTs suspension extracted at 50% strain is about 38.39. The maximum relative resistance of the CT sensor with 10 mL of CNTs suspension extracted was about 59.62. The conductive network of the strain sensor undergoes destruction and reconstruction during stretching and recovery.

A substantial body of research confirms that the formation and expansion of cracks in the conductive network under strain can effectively enhance the sensitivity of the sensors [88, 89]. As the CNTs loading increases, the sensor builds more conductive pathways when not being stretched. When cracks form, the disruption rate of conductive pathways increases significantly, resulting in a noticeable increase in the relative resistance, which contributes to enhancing the sensitivity. However, as the loading of CNTs continues to increase to a certain level, most of the conductive paths still can not be completely disrupted under greater strain. The conductive network, composed of conductive fillers, remains interconnected, resulting in a decrease in the relative resistance. Therefore, it can be considered that the flexible strain sensor filtered with 10 mL of CNTs suspension exhibits good sensing performance and is suitable for various application scenarios.

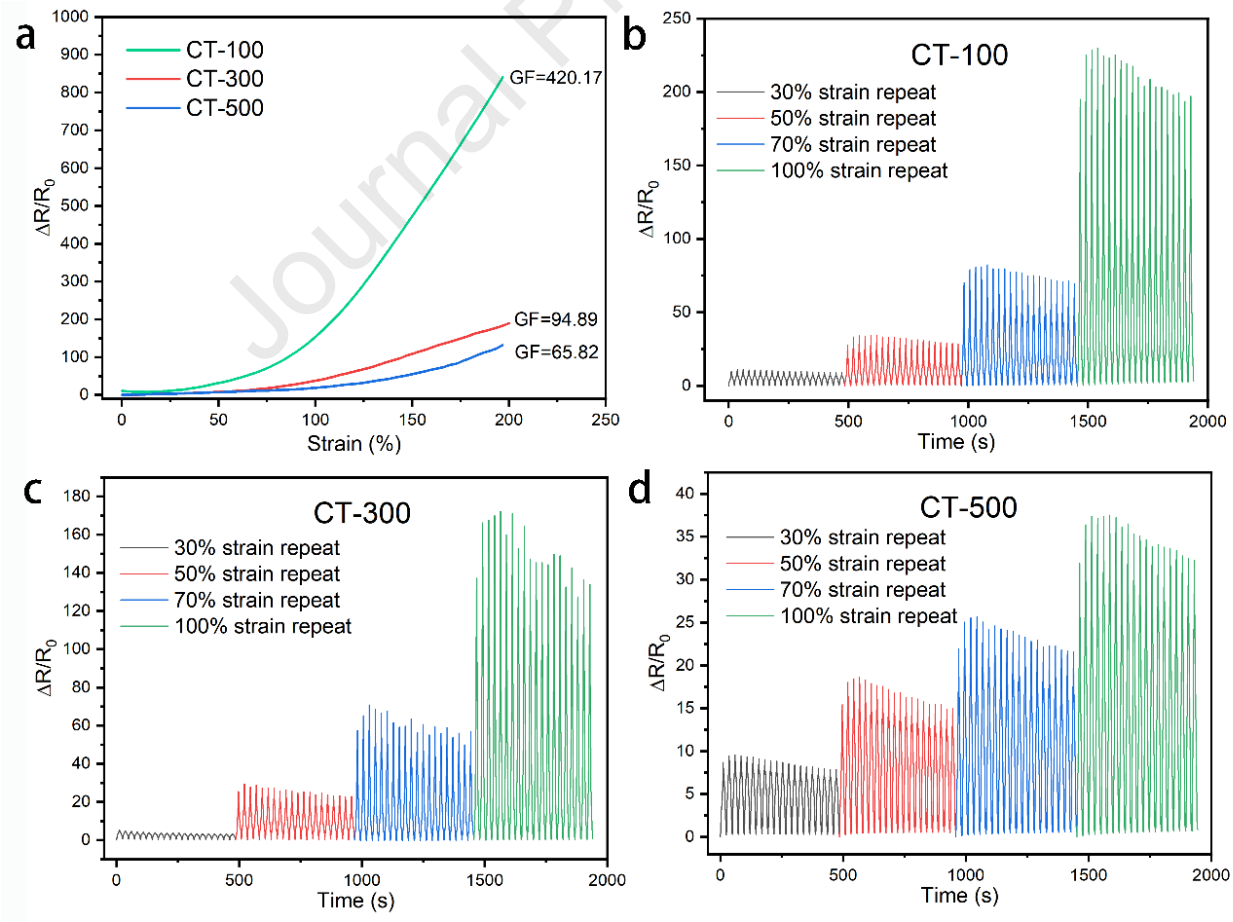

Fig. 7. a. Unidirectional tensile signal response of CT sensors at different speeds. b. CT-100, c. CT-300 and d. CT-500 sensors respond to cyclic electrical signals.

In order to further compare the effects of TPU fiber membrane substrates prepared at different receiving roller speeds on the sensing performance of the fabricated sensors, as shown in Fig. 7a, the electrical signal responses of the sensors prepared on TPU substrates at three different speeds were plotted under 0-200% strain. The CNTs/TPU sensor prepared at receiving roller speeds of 100 r/min, 300 r/min, and 500 r/min were named as CT-100, CT-300 and CT-500, respectively. It can be seen that with the decrease in the receiving roller speed, the fabricated sensors exhibit better resistance responsiveness. Generally speaking, the sensitivity also called gauge factor (GF) of a sensor is an important parameter for evaluating its sensing performance, and is defined as the ratio of relative resistance change to strain, as shown in Equation 2 [90, 91]:

$$GF = (\Delta R / R_0)/\varepsilon \quad (2)$$

where R_0 is the initial resistance of the sensor, ΔR is the difference between the real-time resistance of the sensor and the initial resistance when applying a strain, and ε is the applied strain and is defined as: $\varepsilon = \Delta L / L_0$, where ΔL is the displacement under the strain, L_0 is the initial length.

Through calculations, it is found that the sensitivity of the sensor also increases with the decrease in receiving roller speed. Compared to TPU-based strain sensors prepared using conventional physical blending methods [92], TPU/CNTs strain sensors fabricated via electrospinning demonstrate enhanced sensitivity and a broader stretching range. Specifically, the CT-100 sensor achieves the highest GF value of 420.17 within the 0-200% strain range. This improvement can be attributed to the fabrication of the TPU fiber membrane substrate at a low receiving roller speed, which effectively alleviates the internal stresses, leading to an increased fiber diameters and a more stable scaffold structure. Consequently, this facilitates the incorporation of a higher

quantity of CNTs conductive particles onto the fiber network and the formation of additional conductive pathways. Upon undergoing stretching, a greater number of conductive networks within the sensor are disrupted, resulting in more pronounced resistance changes and heightened sensitivity. Recently, different types of conductive fillers such as CNTs, carbon black , graphene and a combination of fillers such as CNT/graphene, CB/CNT were used to prepare conductive TPU composites for strain-sensing applications [92]. Among them, melt blending and solution processing are typical preparation methods. However, it is difficult to achieve high sensitivity through a simple physical mixing. For example, a study has explored the CNTs/TPU nanocomposites with 2 wt% filler content and reported a gauge factor of 28 under 50% strain [93]. By comparison, the gauge factor of our sensor can exceed 100 at 50% strain.

Fig. 7(b-d) illustrates the electrical signal responses of CT-100, CT-300, and CT-500 sensors over 20 cycles at strain levels of 30%, 50%, 70%, and 100%. It is evident that as the rotational speed decreases, the CT sensor demonstrates generally improved cyclic electrical signal response across various strain levels. However, during cycling at 10% strain, the average relative resistance for CT-100 is approximately 9.31, it is about 3.70 for CT-300, and it is approximately 8.83 for the CT-500 sample. The average relative resistance of the CT-500 sensor is slightly higher than that of the CT-300 sensor. This discrepancy may be attributed to the smaller fiber diameter of the CT-500 sensor and the limited amount of CNTs loaded onto the fiber membrane. When the strain is small, the main factor contributing to the change in relative resistance is the separation of the conductive layer comprised of CNTs. This separation leads to numerous fractures in the conductive network, resulting in a significant alteration in relative resistance. As the strain progressively increases, the conductive path formed by the CNTs loaded on the TPU fiber of both the CT-100 and CT-300 sensors begins to break. This breakage causes a more pronounced change in the relative resistance compared to the CT-500 sensor. According to the figure, it

is evident that the resistance of the CT-300 sample exhibits insufficient stability. This phenomenon may arise from the abundance of fine fibers within the TPU-300, which may disrupt the regularity of the internal conductive network. In conclusion, we propose that the CT-100 sensor exhibits superior sensing capabilities.

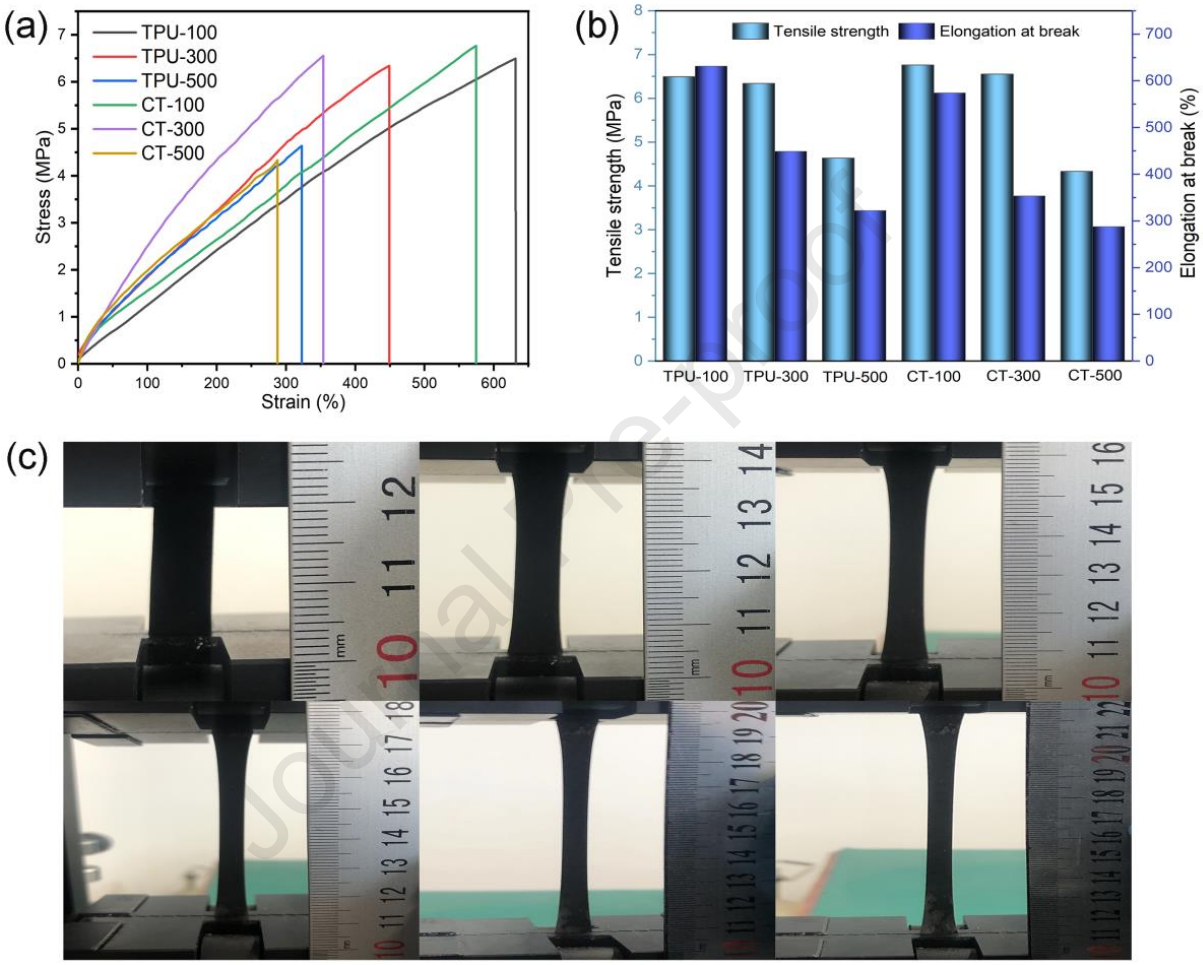

Fig. 8. (a) Unidirectional tensile curve, (b) the tensile strength and elongation at break of samples at different rotational speeds, and (c) the tensile diagram of CT-100 sensor under 0%-600% strain.

The mechanical properties of TPU electrospun fiber membranes and CT sensors prepared at speeds of 100 r/min, 300 r/min, and 500 r/min through uniaxial tensile tests were investigated. The test results are shown in Fig. 8. From Fig. 8a-b, as the rotational speed decreases, both the elongation at break and the tensile strength of the TPU fiber membrane and the prepared CT series sensors gradually increase. The TPU-100 fiber membrane

and CT-100 sensor samples have good mechanical properties, and the tensile strength of the TPU-100 sample increases to about 6.49 MPa.

Compared to the TPU-based strain sensors prepared using traditional physical blending methods [94], the elongation at break of the TPU-100 sample has been significantly increased (632%). This enables the TPU-100 sensor to have a broader strain operating range. Reducing the rotational speed can eliminate internal stress, leading to an increase in the average fiber diameter within the TPU electrospun membrane and a more stable scaffold structure. However, with the introduction of CNTs, the elongation at break of the sample decreases, but the tensile strength slightly increases. Compared to TPU-100, the tensile strength of CT-100 is increased by about 0.27 MPa, and the elongation at break is decreased by about 57%, This may be due to the uniform distribution of the conductive layer constructed by CNTs on the surface of TPU fibers, forming a dense conductive layer, and the presence of hydrogen bonding between CNTs and TPU fiber membranes, which alters their mechanical properties [39].

In summary, we believe that the CT-100 sensor has good mechanical properties and can basically meet the usage requirements of flexible strain sensors under large strains. Fig. 8c shows the actual tensile diagram of the CT-100 sensor under 0%-600% strain, and the sensor can stretch from the initial 2 to 12 cm.

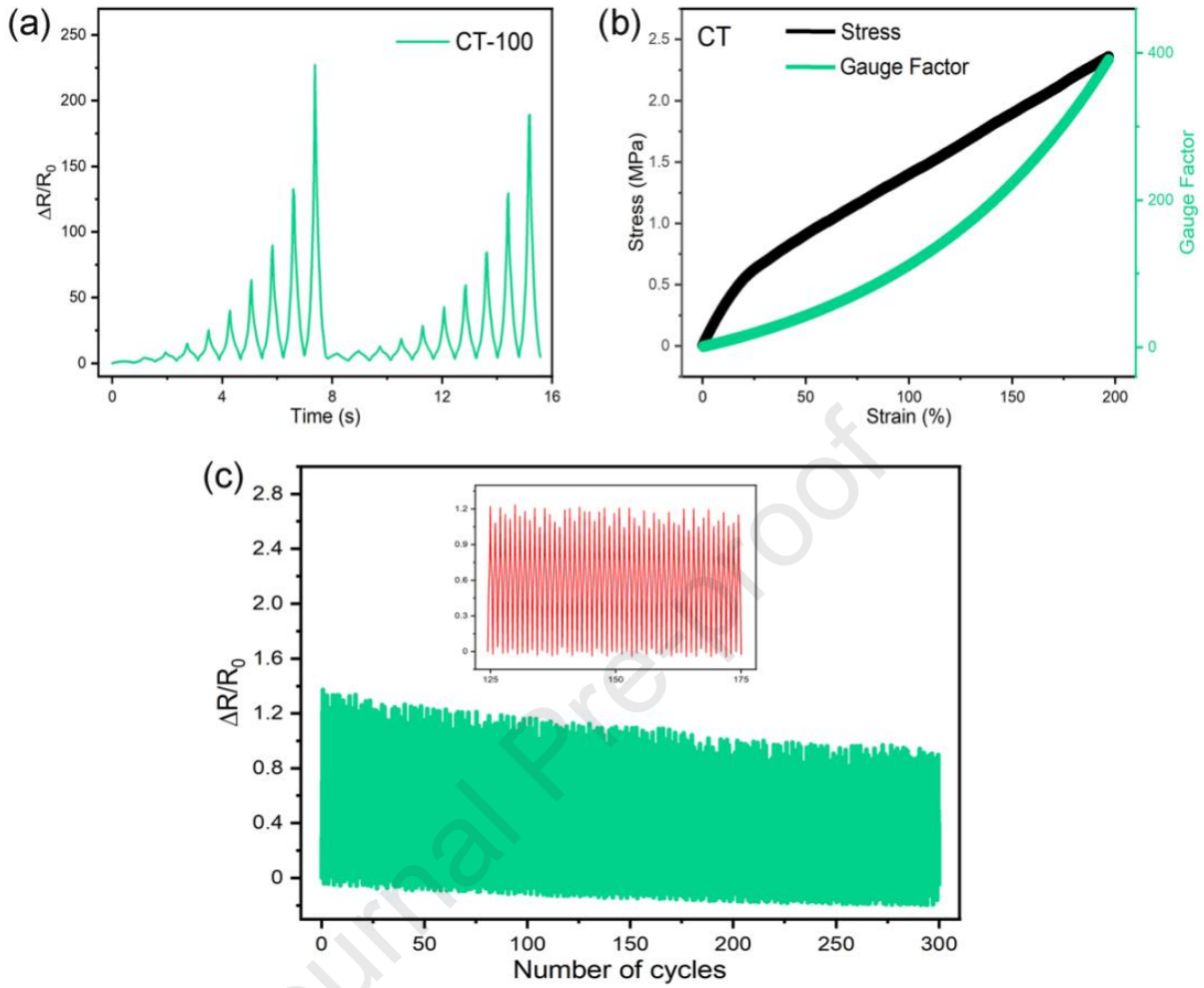

Fig. 9. (a) Two cycle tests of CT-100 sensor tensile under different strains, (b) unit strain sensitivity of CT sensors, and (c) The relative resistance changes of the CT-100 sensor were repeated 300 times at 10% strain.

Fig. 9a shows the two cycle tests of CT-100 samples with a 10% increase in the strain from 10% to 100%. The CT-100 sensor has made accurate responses to each stage of strain, further verifying the good reliability of the CT-100 sensor. Fig. 9b shows the strain of the CT sensor at 0-200% strain at each unit strain, with a maximum value of 399.66, further demonstrating that the prepared CT sensor has good response ability. The CT-100 sensor was subjected to 300 cycles of 10% strain testing at a tensile speed of 100 mm/min to verify its durability and

stability during long-term use. The test results are shown in Fig. 9c. From the figure, the relative resistance of the sensor remained around 2.5 during 300 cycles under 10% strain, and there was no significant difference in relative resistance between stretching and recovery. The results indicate that the CT sensor has good stability during long-term use.

3.3 The application of CT sensors in human motion monitoring

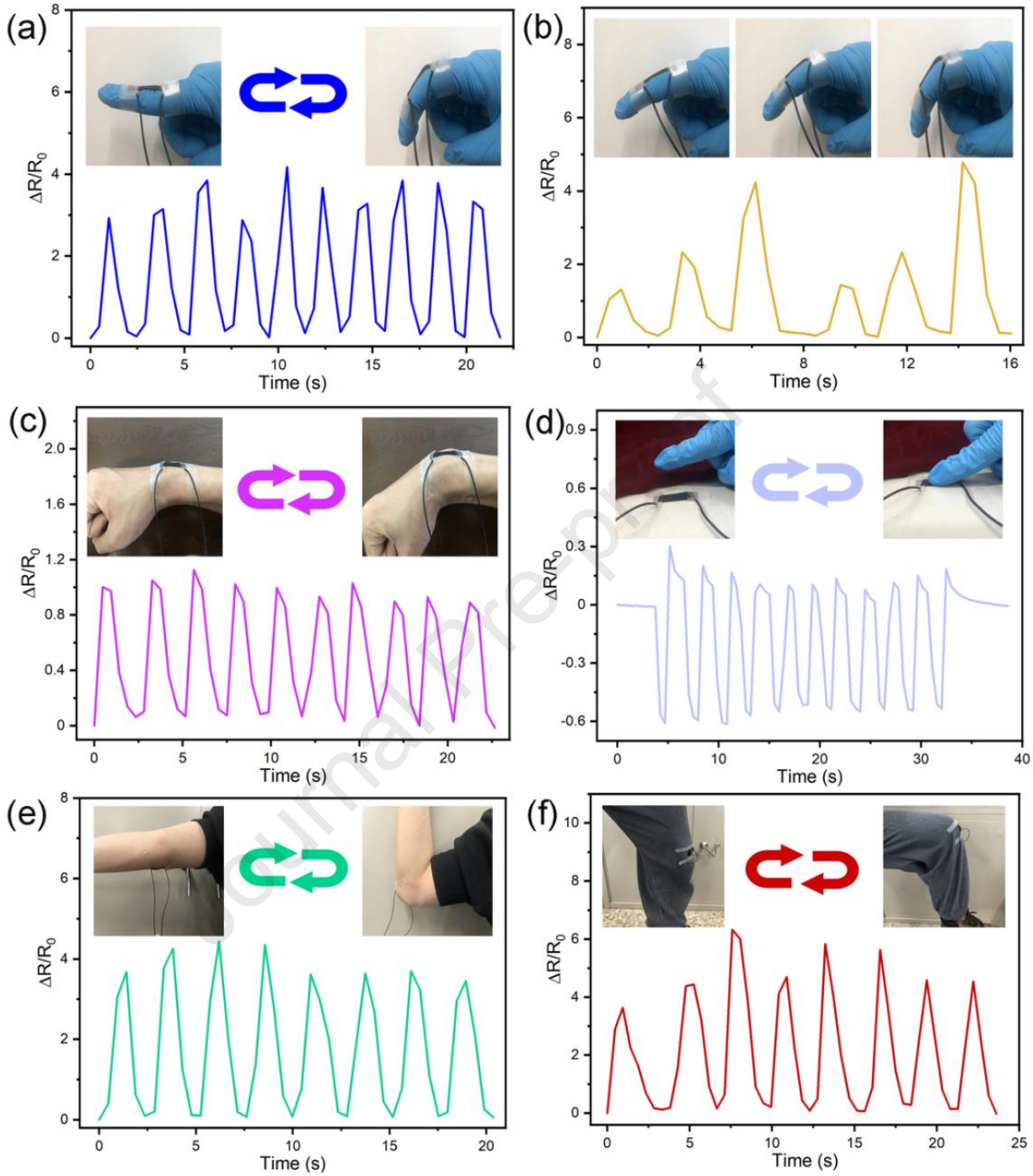

Fig. 10. (a) Flexion of knuckle, (b) the fingers are bent at different angles, (c) wrist flex, (d) finger press, (e) arm bending, and (f) knee bending.

The CT-100 flexible strain sensor prepared according to this article demonstrates good long-term stability, stretchability, and excellent sensing performance. Moreover, the CT-100 sensor has the advantages of simple and

efficient preparation method, lightweight and portable, and can be customized according to the required size. It can be used as a wearable flexible electronic skin for motion monitoring of various parts of the human body. Its working principle is that when the sensor that fits the human skin is subjected to an external stress caused by human movement, the sensor will deform, and the overlap of CNTs in the internal conductive network of the sensor will also change with the effect of external stress, showing a response to human motion electrical signals. The monitoring application of the CT-100 sensor for various human movements is shown in Fig. 10.

As shown in Fig. 10a-b, the relative resistance of the CT-100 sensor gradually increases with the bending of the fingers and returns to its initial position when the fingers return to their original position. It can also make accurate responses when the fingers are bent at 30°, 60°, and 90°, respectively. As shown in Fig. 10c, when the CT-100 sensor is fixed on the volunteer's wrist, the sensor can provide a regular and accurate electrical signal response to the bending of the wrist joint. As shown in Fig. 10d, the CT-100 sensor is able to respond to the finger pressure with electrical signals. When the finger is pressed, the conductive network constructed by the CNTs inside the sensor closely overlaps, showing a decrease in relative resistance. When the pressure is completed, the resistance returns to its initial position. As shown in Fig. 10e-f, the CT-100 sensor responds regularly and accurately to the changes in arm and knee movements.

4. Conclusions

In this study, a high-performance flexible strain sensor was prepared by loading carbon nanotubes (CNTs) onto an electrospun TPU nanofiber membrane. The sensor exhibits unique characteristics such as high sensitivity, a wide detection range, fast response speed, low cost, and a simple fabrication process. Our findings indicate that reducing the rotational speed can eliminate internal stress, leading to an increase in the average fiber diameter within the TPU electrospun membrane and a more stable scaffold structure. This condition facilitates

the loading of more conductive CNT particles on the fiber network and the establishment of additional conductive pathways. The introduction of uniformly distributed CNTs on the surface of TPU fibers forms a dense conductive layer, while the hydrogen bonding between CNTs and TPU fiber membranes could enhance the mechanical strength of the fiber membranes. Finally, a series of performance tests was conducted on the CT-100 sensor. Monitoring the motion signals of each body part demonstrates the excellent performance and practical value of the CT-100 sensor.

Acknowledgements

The authors would like to express their sincere gratitude to the following individuals for their valuable contributions to this research. This work was supported by the Heilongjiang Province Postdoctoral Funded Project (LBH-Q21019), Heilongjiang Province Natural Science Foundation (LH2020E087). The authors extend their appreciation to Taif University, Saudi Arabia for supporting this work through project number (TU-DSPP-2024-99).

Author contributions

Zijian Wu, Xuesong Deng and Xin Yu: Concept, investigation, formal analysis, writing—original draft. Junwei Gu and Hongyu Xu: data curation, methodology, writing—review and editing. Zeinhom M. El-Bahy, Jing Zhang, Gaber A. M. Mersal, Junguo Gao: Resources, data analysis, writing—review and editing. A. Alhadhrami: writing – review and editing; Ning Guo, Ling Weng and Zhanhu Guo: Concept, supervision, resources, writing—review and editing.

Data availability statement

Data will be available upon request.

Declarations

Conflict of interest the authors declare no competing interests.

References

[1] C. Li, Towards conductive hydrogels in e-skins: a review on rational design and recent developments, RSC Adv. 11(54) (2021) 33835-33848.
[2] X. Yuan, C. Li, X. Yin, Y. Yang, B. Ji, Y. Niu, L. Ren, Epidermal wearable biosensors for monitoring biomarkers of chronic disease in sweat, Biosensors 13(3) (2023) 313.
[3] J. Zhang, Y. Wang, Q. Wei, M. Li, X. Chen, 3D printable, stretchable, anti-freezing and rapid self-healing organogel-based sensors for human motion detection, J. Colloid Interface Sci. 653 (2024) 1514-1525.
[4] X. Wang, Y. Shen, S. Xu, C. Huang, C. Lai, Q. Yong, F. Chu, H. Algadi, D. Zhang, C. Lu, J. Wang, Lignin in situ self-assembly facilitates biomimetic multiphase structure for fabricating ultra-strong and tough ionic conductors for wearable pressure and strain sensors, Adv. Comp. Hybrid Mater. 6(3) (2023) 84.
[5] C. Hu, F. Wang, X. Cui, Y. Zhu, Recent progress in textile-based triboelectric force sensors for wearable electronics, Adv. Compos. Hybrid Mater. 6(2) (2023) 70.
[6] Y. Chen, G. Li, W. Mu, X. Wan, D. Lu, J. Gao, D. Wen, Nonenzymatic sweat wearable uric acid sensor based on N-doped reduced graphene oxide/Au dual aerogels, Ana. Chem. 95(7) (2023) 3864-3872.
[7] Y. Jiang, A. Hu, W. Feng, Y. Chen, M. Ai, D. Yu, W. Wang, Non-covalent crosslinked hydrogels to realize renewable and re-moldable strain sensors with excellent sensing behavior, Polymer 290 (2024) 126588.
[8] A. Balakrishnan, J. Medikonda, P.K. Namboothiri , M. Manik, a. Natarajan, Role of wearable sensors with machine learning approaches in gait analysis for Parkinson's disease assessment: A review, Eng. Sci. 19 (2022) 5-19.
[9] T. Shen, S. Liu, X. Yue, Z. Wang, H. Liu, R. Yin, C. Liu, C. Shen, High-performance fibrous strain sensor with synergistic sensing layer for human motion recognition and robot control, Adv. Comp. Hybrid Mater. 6(4) (2023) 127.
[10] C. Liu, L. Jiang, O. Yue, Y. Feng, B. Zeng, Y. Wu, Y. Wang, J. Wang, L. Zhao, X. Wang, C. Shao, Q. Wu, X. Sun, Thermal enhancement of gelatin hydrogels for a multimodal sensor and self-powered triboelectric nanogenerator at low temperatures, Adv. Compos. Hybrid Mater. 6(3) (2023) 112.
[11] D.-E. Wang, X. Gao, S. You, M. Chen, L. Ren, W. Sun, H. Yang, H. Xu, Aptamer-functionalized polydiacetylene liposomes act as a fluorescent sensor for sensitive detection of MUC1 and targeted imaging of cancer cells, Sensors Actuators B: Chem. 309 (2020) 127778.
[12] Z. Ma, S. Cheng, W. Kou, H. Chen, W. Wang, X. Zhang, T. Guo, Sensitivity-enhanced extrinsic Fabry–Perot interferometric fiber-optic microcavity strain sensor, Sensors 19(19) (2019) 4097.
[13] J. Huang, Y. Liu, J. Lin, J. Su, C. Redshaw, X. Feng, Y. Min, Novel pyrene-based aggregation-induced emission luminogen (AIEgen) composite phase change fibers with satisfactory fluorescence anti-counterfeiting, temperature sensing, and high-temperature warning functions for solar-thermal energy storage, Adv. Compos. Hybrid Mater. 6(4) (2023) 126.
[14] Q. Wang, J. Zeng, J. Li, S. Yu, M.T. Innocent, M. Li, W. Ma, H. Xiang, M. Zhu, Multifunctional fiber derived from wet spinning combined with UV photopolymerization for human motion and temperature detection, Adv. Compos. Hybrid Mater. 6(1) (2022) 26.
[15] G. Li, J. Hao, W. Li, F. Ma, T. Ma, W. Gao, Y. Yu, D. Wen, Integrating highly porous and flexible Au hydrogels with soft-MEMS technologies for high-performance wearable biosensing, Ana. Chem. 93(42) (2021) 14068-14075.

[16] H. Li, H. Fan, Z. Liu, J. Zhang, Y. Wen, J. Lu, X. Jiang, G. Chen, Highly sensitive humidity sensor based on lithium stabilized Na-β"-alumina: dc and ac analysis, Sens. Actuators B: Chem. 255 (2018) 1445-1454.
[17] Y. Ge, J. Zeng, B. Hu, D.-Y. Yang, Y. Shao, H. Lu, Bioinspired flexible film as intelligent moisture-responsive actuators and noncontact sensors, Giant 11 (2022) 100107.
[18] S. Yan, D. Shen, B. Xin, M.A.A. Newton, Y. Wu, Rhombus-patterned flexible self-supported PVDF-based humidity sensor for respiratory monitoring, Polymer 282 (2023) 126139.
[19] D. Zhang, M. Zhang, J. Wang, H. Sun, H. Liu, L. Mi, C. Liu, C. Shen, Impedance response behavior and mechanism study of axon-like ionic conductive cellulose-based hydrogel strain sensor, Adv. Compos. Hybrid Mater. 5(3) (2022) 1812-1820.
[20] Y. Liu, J. Wang, J. Chen, Q. Yuan, Y. Zhu, Ultrasensitive iontronic pressure sensor based on rose-structured ionogel dielectric layer and compressively porous electrodes, Adv. Compos. Hybrid Mater. 6(6) (2023) 210.
[21] Y. Wu, J. Wu, Y. Lin, J. Liu, X. Pan, X. He, K. Bi, M. Lei, Melamine sponge skeleton loaded organic conductors for mechanical sensors with high sensitivity and high resolution, Adv. Compos. Hybrid Mater. 6(1) (2022) 4.
[22] H. Zhou, Y. Zhang, Y. Qiu, H. Wu, W. Qin, Y. Liao, Q. Yu, H. Cheng, Stretchable piezoelectric energy harvesters and self-powered sensors for wearable and implantable devices, Biosen. Bioelectronics 168 (2020) 112569.
[23] J. Liu, E. Chen, Y. Wu, H. Yang, K. Huang, G. Chang, X. Pan, K. Huang, Z. He, M. Lei, Silver nanosheets doped polyvinyl alcohol hydrogel piezoresistive bifunctional sensor with a wide range and high resolution for human motion detection, Adv. Compos. Hybrid Mater. 5(2) (2022) 1196-1205.
[24] S. Shi, W. Xu, B. Zhou, S. Qin, X. Liu, H. Li, Low-density polyethylene-multi-walled carbon nanotube nanocomposite membranes with enhanced conductivity for highly sensitive vapor sensing, Adv. Compos. Hybrid Mater. 6(5) (2023) 168.
[25] Y. Wang, L. Ma, W. Li, A.M. Deibel, W. Li, H. Tian, X. Liu, NiO-based sensor for in situ CO monitoring above 1000 °C: behavior and mechanism, Adv. Compos. Hybrid Mater. 5(3) (2022) 2478-2490.
[26] J. Ma, H. Fan, W. Zhang, J. Sui, C. Wang, M. Zhang, N. Zhao, A. Kumar Yadav, W. Wang, W. Dong, S. Wang, High sensitivity and ultra-low detection limit of chlorine gas sensor based on In2O3 nanosheets by a simple template method, Sens. Actuators B: Chem. 305 (2020) 127456.
[27] F. Li, Z. Zeng, M. Wu, L. Liu, W. Li, F. Huang, W. Li, H. Guan, W. Geng, Room-temperature triethylamine sensing of a chemiresistive sensor based on Sm-doped SnS2/ZnS hierarchical microspheres, New J. Chem. 46(32) (2022) 15701-15711.
[28] R.D. Prasad, R.S. Prasad, Y.I. Shaikh, S.R. Prasad, M.N. Padvi, P.D. Sarvalkar, S. Saxena, V.S. Shaikh, G.M. Nazeruddin, S. Shaikh, A.B. Kanwade, N. Charmode, A.K. Vaidya, O.P. Shrivastav, C.B. Desai, P.D. Patil, A critical review on uses of gases in veterinary medicine and gas sensing materials, ES Mater. Manuf. 23 (2024) 1084.
[29] B. Jiang, K. Zhou, C. Wang, Q. Sun, G. Yin, Z. Tai, K. Wilson, J. Zhao, L. Zhang, Label-free glucose biosensor based on enzymatic graphene oxide-functionalized tilted fiber grating, Sens. Actuators B: Chem. 254 (2018) 1033-1039.
[30] M. Gijare, S. Chaudhari, S. Ekar, A. Garje, Reduced graphene oxide based electrochemical nonenzymatic human serum glucose sensor, ES Mater. Manuf. 14 (2021) 110-119.
[31] L. Zhu, Q. Wu, X. Mei, Y. Li, J. Yang, Paper-based microfluidic sensor array for tetracycline antibiotics discrimination using lanthanide metal–carbon quantum dots composite ink, Adv. Compos. Hybrid Mater. 6(6) (2023) 221.

[32] J. Ma, H. Fan, Z. Li, Y. Jia, A.K. Yadav, G. Dong, W. Wang, W. Dong, S. Wang, Multi-walled carbon nanotubes/polyaniline on the ethylenediamine modified polyethylene terephthalate fibers for a flexible room temperature ammonia gas sensor with high responses, Sens. Actuators B: Chem. 334 (2021) 129677.
[33] J. Lu, X. Zhang, X. Zhang, N. Liu, H. Li, Z. Yu, X. Yan, Electrochemical sensor for mercuric chloride based on graphene-MnO2 composite as recognition element, Electroch. Acta 174 (2015) 221-229.
[34] J. Chen, L. Wang, X. Xu, G. Liu, H. Liu, Y. Qiao, J. Chen, S. Cao, Q. Cha, T. Wang, Self-healing materials-based electronic skin: mechanism, development and applications, Gels 8(6) (2022) 356.
[35] Y. He, M. Zhou, M.H.H. Mahmoud, X. Lu, G. He, L. Zhang, M. Huang, A.Y. Elnaggar, Q. Lei, H. Liu, C. Liu, I.H.E. Azab, Multifunctional wearable strain/pressure sensor based on conductive carbon nanotubes/silk nonwoven fabric with high durability and low detection limit, Adv. Compos. Hybrid Mater. 5(3) (2022) 1939-1950.
[36] F. Ramirez-Gonzalez, G. Garcia-Salgado, E. Rosendo, T. Diaz, F. Nieto-Caballero, A. Coyopol, R. Romano, A. Luna, K. Monfil, E. Gastellou, Porous silicon gas sensors: the role of the layer thickness and the silicon conductivity, Sensors (Basel) 20(17) (2020).
[37] G. Li, D. Wen, Sensing nanomaterials of wearable glucose sensors, Chinese Chemical Letters 32(1) (2021) 221-228.
[38] M. Amit, L. Chukoskie, A.J. Skalsky, H. Garudadri, T.N. Ng, Flexible pressure sensors for objective assessment of motor disorders, Adv. Funct. Mater. 30(20) (2020).
[39] X. Wang, X. Liu, D.W. Schubert, Highly sensitive ultrathin flexible thermoplastic polyurethane/carbon black fibrous film strain sensor with adjustable scaffold networks, Nanomicro Lett. 13(1) (2021) 64.
[40] T. Yamada, Y. Hayamizu, Y. Yamamoto, Y. Yomogida, A. Izadi-Najafabadi, D.N. Futaba, K. Hata, A stretchable carbon nanotube strain sensor for human-motion detection, Nat. Nanotechnol. 6(5) (2011) 296-301.
[41] D.H. Kim, N. Lu, R. Ma, Y.S. Kim, R.H. Kim, S. Wang, J. Wu, S.M. Won, H. Tao, A. Islam, K.J. Yu, T.I. Kim, R. Chowdhury, M. Ying, L. Xu, M. Li, H.J. Chung, H. Keum, M. McCormick, P. Liu, Y.W. Zhang, F.G. Omenetto, Y. Huang, T. Coleman, J.A. Rogers, Epidermal electronics, Science 333(6044) (2011) 838-43.
[42] B. Wang, A. Facchetti, Mechanically flexible conductors for stretchable and wearable E-skin and E-textile devices, Adv. Mater. 31(28) (2019) e1901408.
[43] J.C. Yang, J. Mun, S.Y. Kwon, S. Park, Z. Bao, S. Park, Electronic skin: recent progress and future prospects for skin-attachable devices for health monitoring, robotics, and prosthetics, Adv. Mater. 31(48) (2019) e1904765.
[44] H. Joo, Y. Lee, J. Kim, J.S. Yoo, S. Yoo, S. Kim, A.K. Arya, S. Kim, S.H. Choi, N. Lu, H.S. Lee, S. Kim, S.T. Lee, D.H. Kim, Soft implantable drug delivery device integrated wirelessly with wearable devices to treat fatal seizures, Sci. Adv. 7(1) (2021) eabd4639.
[45] Z. Lou, L.L. Wang, K. Jiang, Z.M. Wei, G.Z. Shen, Reviews of wearable healthcare systems: Materials, devices and system integration, Mat. Sci. Eng. R 140 (2020).
[46] S. Wang, T. Chinnasamy, M.A. Lifson, F. Inci, U. Demirci, Flexible substrate-based devices for point-of-care diagnostics, Trends Biotechnol. 34(11) (2016) 909-921.
[47] K. Xu, Y. Fujita, Y. Lu, S. Honda, M. Shiomi, T. Arie, S. Akita, K. Takei, A wearable body condition sensor system with wireless feedback alarm functions, Adv. Mater. 33(18) (2021) e2008701.
[48] D. Sarkar, N. Das, M.M. Saikh, S. Roy, S. Paul, N.A. Hoque, R. Basu, S. Das, Elevating the performance of nanoporous bismuth selenide incorporated arch-shaped triboelectric nanogenerator by implementing piezo-tribo coupling effect: harvesting biomechanical energy and low scale energy sensing applications, Adv. Compos. Hybrid Mater. 6(6) (2023) 232.

[49] S. Sharafkhani, M. Kokabi, Enhanced sensing performance of polyvinylidene fluoride nanofibers containing preferred oriented carbon nanotubes, Adv. Compos. Hybrid Mater. 5(4) (2022) 3081-3093.
[50] K. Fan, K. Li, L. Han, Z. Yang, J. Yang, J. Zhang, J. Cheng, Multifunctional double-network Ti3C2Tx MXene composite hydrogels for strain sensors with effective electromagnetic interference and UV shielding properties, Polymer 273 (2023) 125865.
[51] Z.M. Chu, W.C. Jiao, Y.F. Huang, Y.T. Zheng, R.G. Wang, X.D. He, Superhydrophobic gradient wrinkle strain sensor with ultra-high sensitivity and broad strain range for motion monitoring, J. Mater. Chem. A 9(15) (2021) 9634-9643.
[52] R. Liu, J.G. Kim, P. Dhakal, W. Li, J. Ma, A. Hou, C. Merkel, J. Qiu, M. Zoran, S. Wang, Neuromorphic properties of flexible carbon nanotube/polydimethylsiloxane nanocomposites, Adv. Compos. Hybrid Mater. 6(1) (2022) 14.
[53] Z. Qin, W. Xu, D. Wang, Y. Jiang, L. Zhu, X. Chen, Y. Li, X. Zhang, C. Jia, B.B. Xu, Mechanics of micropattern-guided formation of elastic surface instabilities on the polydimethylsiloxane bilayer, Adv. Compos. Hybrid Mater. 6(5) (2023) 160.
[54] H. Zhang, X. Zhang, D. Li, J. Zhuang, Y. Liu, H. Liu, D. Wu, J. Feng, J. Sun, Synergistic enhanced thermal conductivity of polydimethylsiloxane composites via introducing SCF and hetero-structured GB@rGO hybrid fillers, Adv. Compos. Hybrid Mater. 5(3) (2022) 1756-1768.
[55] X.M. Zhang, X.L. Yang, K.Y. Wang, Conductive graphene/polydimethylsiloxane nanocomposites for flexible strain sensors, J. Mater. Sci.-Mater. Electron. 30(21) (2019) 19319-19324.
[56] Y. Gao, X.L. Fang, J.P. Tan, T. Lu, L.K. Pan, F.Z. Xuan, Highly sensitive strain sensors based on fragmentized carbon nanotube/polydimethylsiloxane composites, Nanotechnology 29(23) (2018) 235501.
[57] Z. Cui, S.s.a. Marcelle, M. Zhao, J. Wu, X. Liu, J. Si, Q. Wang, Thermoplastic polyurethane/titania/polydopamine(TPU/TiO2/PDA) 3-D porous composite foam with outstanding oil/water separation performance and photocatalytic dye degradation, Adv. Compos. Hybrid Mater.5(4) (2022) 2801-2816.
[58] J.-W. Li, B.-S. Huang, C.-H. Chang, C.-W. Chiu, Advanced electrospun AgNPs/rGO/PEDOT:PSS/TPU nanofiber electrodes: Stretchable, self-healing, and perspiration-resistant wearable devices for enhanced ECG and EMG monitoring, Adv. Compos. Hybrid Mater. 6(6) (2023) 231.
[59] Y. Shen, W. Yang, F. Hu, X. Zheng, Y. Zheng, H. Liu, H. Algadi, K. Chen, Ultrasensitive wearable strain sensor for promising application in cardiac rehabilitation, Adv. Compos. Hybrid Mater. 6(1) (2022) 21.
[60] I.A. Rashid, M.S. Irfan, Y.Q. Gill, R. Nazar, F. Saeed, A. Afzal, H. Ehsan, A.A. Qaiser, A. Shakoor, Stretchable strain sensors based on polyaniline/thermoplastic polyurethane blends, Polym. Bull. 77(3) (2020) 1081-1093.
[61] Y.L. Fang, J.H. Xu, F. Gao, X.S. Du, Z.L. Du, X. Cheng, H.B. Wang, Self-healable and recyclable polyurethane-polyaniline hydrogel toward flexible strain sensor, Compos. Part B-Eng. 219 (2021) 108965.
[62] Y. Luo, G. Zhao, J. Chen, X. Chang, J. Huang, Y. Zhu, Lightweight and highly compressible/stretchable ionogel foams for designing pressure and strain sensors, Polymer 293 (2024) 126616.
[63] M. Xu, J. Qi, F. Li, Y. Zhang, Highly stretchable strain sensors with reduced graphene oxide sensing liquids for wearable electronics, Nanoscale 10(11) (2018) 5264-5271.
[64] J. Liu, K. Liu, X. Pan, K. Bi, F. Zhou, P. Lu, M. Lei, A flexible semidry electrode for long-term, high-quality electrocardiogram monitoring, Adv. Compos. Hybrid Mater. 6(1) (2022) 13.
[65] Y. Wang, Y. Yu, F. Zhao, Y. Feng, W. Feng, Multi-functional and multi-responsive layered double hydroxide-reinforced polyacrylic acid composite hydrogels as ionic skin sensors, Adv. Compos. Hybrid Mater. 6(2) (2023) 65.

[66] X.-Q. Zhan, Z.-Q. Ran, H.-Y. Bao, Q. Ye, H. Chen, Q. Fu, W. Ni, J.-M. Xu, N. Ma, F.-C. Tsai, Intelligent hydrogel on–off controller sensor for irrigation, Adv. Compos. Hybrid Mater. 7(1) (2023) 6.
[67] H. Wang, L. Meng, Y. Ye, J. Wu, S. Zhu, Y. Liu, K. Li, X. Yang, M. Wei, M. Wang, L. Song, S. Guo, Antibacterial zwitterionic hydrogel for flexible and wearable ultrafast-response strain sensors with low hysteresis, Giant 17 (2024) 100234.
[68] L. Liu, Y. Chen, C. Zhao, M. Guo, Y. Wu, Y. Li, D. Xiang, H. Li, L. Wang, X. Zhang, Highly sensitive, super high stretchable hydrogel strain sensor with underwater repeated adhesion and rapid healing, Polymer 285 (2023) 126317.
[69] H. Nesser, J. Grisolia, T. Alnasser, B. Viallet, L. Ressier, Towards wireless highly sensitive capacitive strain sensors based on gold colloidal nanoparticles, Nanoscale 10(22) (2018) 10479-10487.
[70] S.B. Choi, J.S. Meena, J. Joo, J.-W. Kim, Autonomous self-healing wearable flexible heaters enabled by innovative MXene/polycaprolactone composite fibrous networks and silver nanowires, Adv. Compos. Hybrid Mater. 6(6) (2023) 227.
[71] G.J. Zhu, P.G. Ren, H. Guo, Y.L. Jin, D.X. Yan, Z.M. Li, Highly Sensitive and Stretchable Polyurethane Fiber Strain Sensors with Embedded Silver Nanowires, ACS Appl. Mater. Interfaces 11(26) (2019) 23649-23658.
[72] X. Zhao, J. Li, M. Jiang, W. Zhai, K. Dai, C. Liu, C. Shen, Flexible strain sensor based on CNTs/CB/TPU conductive fibrous film with wide sensing range and high sensitivity for human biological signal acquisition, Polymer 302 (2024) 127049.
[73] Y. He, Y. Li, X. Liao, L. Li, Interfacial modification strategy for the fabrication of high performance fiber-based strain sensors, Polymer 260 (2022) 125376.
[74] X. Zheng, J. Shen, Q. Hu, W. Nie, Z. Wang, L. Zou, C. Li, Vapor phase polymerized conducting polymer/MXene textiles for wearable electronics, Nanoscale 13(3) (2021) 1832-1841.
[75] M.H. Cao, J. Su, S.Q. Fan, H.W. Qiu, D.L. Su, L. Li, Wearable piezoresistive pressure sensors based on 3D graphene, Chem. Eng. J. 406 (2021).
[76] J.C. Dong, D. Wang, Y.D. Peng, C. Zhang, F.L. Lai, G.J. He, P.M. Ma, W.F. Dong, Y.P. Huang, I.P. Parkin, T.X. Liu, Ultra-stretchable and superhydrophobic textile-based bioelectrodes for robust self-cleaning and personal health monitoring, Nano Energy 97 (2022) 107160.
[77] M. Qu, H. Wang, Q. Chen, L. Wu, P. Tang, M. Fan, Y. Guo, H. Fan, Y. Bin, A thermally-electrically double-responsive polycaprolactone – thermoplastic polyurethane/multi-walled carbon nanotube fiber assisted with highly effective shape memory and strain sensing performance, Chem. Eng. J. 427 (2022).
[78] D. Kanzhigitova, P. Askar, A. Tapkharov, V. Kudryashov, M. Abutalip, R. Rakhmetullayeva, S. Adilov, N. Nuraje, p-Toluenesulfonic acid doped vanadium pentoxide/polypyrrole film for highly sensitive hydrogen sensor, Adv. Compos. Hybrid Mater. 6(6) (2023) 218.
[79] P. Xue, J. Wang, X. Tao, Flexible textile strain sensors from polypyrrole-coated XLA™ elastic fibers, High Perform. Polym. 26(3) (2014) 364-370.
[80] H. Qie, Z. Wang, J. Ren, S. Lü, M. Liu, A tough shape memory hydrogel strain sensor based on gelatin grafted polypyrrole, Polymer 263 (2022) 125524.
[81] F. Bhatti, D. Xiao, T. Jebagu, X. Huang, E. Witherspoon, P. Dong, S. Lei, J. Shen, Z. Wang, Semiconductive biocomposites enabled portable and interchangeable sensor for early osteoarthritis joint inflammation detection, Adv. Compos. Hybrid Mater. 6(1) (2023) 33.

[82] X.M. Li, T.T. Yang, Y. Yang, J. Zhu, L. Li, F.E. Alam, X. Li, K.L. Wang, H.Y. Cheng, C.T. Lin, Y. Fang, H.W. Zhu, Large-Area Ultrathin Graphene Films by Single-Step Marangoni Self-Assembly for Highly Sensitive Strain Sensing Application, Adv. Funct. Mater. 26(9) (2016) 1322-1329.
[83] J. Lin, Z. Yao, M. Xiong, J. Lin, F. Hu, X. Wei, S. Huang, Directional transport of drug droplets based on structural and wettability gradients on antibacterial Janus wound plaster with hemostatic, antiextravasation, and prehealing properties, Adv. Compos. Hybrid Mater. 6(6) (2023) 193.
[84] R.M. Schofield, B.M. Maciejewska, S. Dong, G.T. Tebbutt, D. McGurty, R.S. Bonilla, H.E. Assender, N. Grobert, Driving fiber diameters to the limit: nanoparticle-induced diameter reductions in electrospun photoactive composite nanofibers for organic photovoltaics, Adv. Compos. Hybrid Mater. 6(6) (2023) 229.
[85] J. Li, Y. Zhao, X. Zhao, W. Zhai, K. Dai, C. Liu, C. Shen, Liquid metal-facilitated flexible electrospun thermoplastic polyurethane fibrous mats with aligned wavelike structure for strain and triboelectric double-mode sensing, Compos. Part A: Appl. Sci. Manuf. 179 (2024) 108031.
[86] T. Kuang, M. Zhang, F. Chen, Y. Fei, J. Yang, M. Zhong, B. Wu, T. Liu, Creating poly(lactic acid)/carbon nanotubes/carbon black nanocomposites with high electrical conductivity and good mechanical properties by constructing a segregated double network with a low content of hybrid nanofiller, Adv. Compos. Hybrid Mater. 6(1) (2023) 48.
[87] X. Wang, M. Qu, K. Wu, D.W. Schubert, X. Liu, High sensitive electrospun thermoplastic polyurethane/carbon nanotubes strain sensor fitting by a novel optimization empirical model, Adv. Compos. Hybrid Mater. 6(2) (2023) 63.
[88] E. Aslanidis, E. Skotadis, D. Tsoukalas, Resistive crack-based nanoparticle strain sensors with extreme sensitivity and adjustable gauge factor, made on flexible substrates, Nanoscale 13(5) (2021) 3263-3274.
[89] Y. Wang, F. Wang, S. Yazigi, D. Zhang, X. Gui, Y. Qi, J. Zhong, L. Sun, Nanoengineered highly sensitive and stable soft strain sensor built from cracked carbon nanotube network/composite bilayers, Carbon 173 (2021) 849-856.
[90] J.R. Garcia, D. O'Suilleabhain, H. Kaur, J.N. Coleman, A simple model relating gauge factor to filler loading in nanocomposite strain sensors, ACS Applied Nano Mater. 4(3) (2021) 2876-2886.
[91] M. Cui, S. Wu, J. Li, Y. Zhao, W. Zhai, K. Dai, C. Liu, C. Shen, An ultrasensitive flexible strain sensor based on CNC/CNTs/MXene/TPU fibrous mat for human motion, sound and visually personalized rehabilitation training monitoring, Compos. Sci. Technol. 244 (2023) 110309.
[92] S. Kumar, T.K. Gupta, K. Varadarajan, Strong, stretchable and ultrasensitive MWCNT/TPU nanocomposites for piezoresistive strain sensing, Compos. Part B: Eng. 177 (2019) 107285.
[93] K. Ke, V.S. Bonab, D. Yuan, I. Manas-Zloczower, Piezoresistive thermoplastic polyurethane nanocomposites with carbon nanostructures, Carbon 139 (2018) 52-58.
[94] P. Slobodian, R. Danova, R. Olejnik, J. Matyas, L. Münster, Multifunctional flexible and stretchable polyurethane/carbon nanotube strain sensor for human breath monitoring, Polym. Adv. Technol. 30(7) (2019) 1891-1898.

Highlights

- Electrospinning combined with vacuum filtration was used to prepare strain sensors.
- The influence of manufacturing process parameters on sensor performance was explored.
- The sensor exhibits high sensitivity and excellent mechanical performance.
- The sensor demonstrates good stability.
- The sensor is capable of effectively monitoring human movement.

Declaration of interests

☒ The authors declare that they have no known competing financial interests or personal relationships that could have appeared to influence the work reported in this paper.

☐The authors declare the following financial interests/personal relationships which may be considered as potential competing interests: